

Purdue University Purdue e-Pubs

Birck and NCN Publications

Birck Nanotechnology Center

3-4-2013

Laser direct writing of silicon field effect transistor sensors

Woongsik Nam

Birck Nanotechnology Center, Purdue University, namw@purdue.edu

James I. Mitchell

Birck Nanotechnology Center, Purdue University, jimitche@purdue.edu

Chookiat Tansarawiput

Birck Nanotechnology Center, Purdue University, ctansara@purdue.edu

Minghao Qi

Birck Nanotechnology Center, Purdue University, mqi@purdue.edu

Xianfan Xu

Birck Nanotechnology Center, Purdue University, xxu@purdue.edu

Follow this and additional works at: <http://docs.lib.purdue.edu/nanopub>

 Part of the [Nanoscience and Nanotechnology Commons](#)

Nam, Woongsik; Mitchell, James I.; Tansarawiput, Chookiat; Qi, Minghao; and Xu, Xianfan, "Laser direct writing of silicon field effect transistor sensors" (2013). *Birck and NCN Publications*. Paper 1368.

<http://dx.doi.org/10.1063/1.4794147>

This document has been made available through Purdue e-Pubs, a service of the Purdue University Libraries. Please contact epubs@purdue.edu for additional information.

Laser direct writing of silicon field effect transistor sensors

Woongsik Nam, James I. Mitchell, Chookiat Tansarawiput, Minghao Qi, and Xianfan Xu

Citation: *Appl. Phys. Lett.* **102**, 093504 (2013); doi: 10.1063/1.4794147

View online: <http://dx.doi.org/10.1063/1.4794147>

View Table of Contents: <http://apl.aip.org/resource/1/APPLAB/v102/i9>

Published by the AIP Publishing LLC.

Additional information on *Appl. Phys. Lett.*

Journal Homepage: <http://apl.aip.org/>

Journal Information: http://apl.aip.org/about/about_the_journal

Top downloads: http://apl.aip.org/features/most_downloaded

Information for Authors: <http://apl.aip.org/authors>

ADVERTISEMENT



Laser direct writing of silicon field effect transistor sensors

Woongsik Nam,^{1,2} James I. Mitchell,^{1,2} Chookiat Tansarawiput,^{2,3} Minghao Qi,^{2,3} and Xianfan Xu^{1,2,a)}

¹*School of Mechanical Engineering, Purdue University, West Lafayette, Indiana 47907, USA*

²*Birck Nanotechnology Center, Purdue University, West Lafayette, Indiana 47907, USA*

³*School of Electrical and Computer Engineering, Purdue University, West Lafayette, Indiana 47907, USA*

(Received 30 November 2012; accepted 19 February 2013; published online 4 March 2013)

We demonstrate a single step technique to fabricate silicon wires for field effect transistor sensors. Boron-doped silicon wires are fabricated using laser direct writing in combination with chemical vapor deposition, which has the advantages of precise control of position, orientation, and length, and *in situ* doping. The silicon wires can be fabricated to have very rough surfaces by controlling laser operation parameters, and thus, have large surface areas, enabling high sensitivity for sensing. Highly sensitive pH sensing is demonstrated. We expect our method can be expanded to the fabrication of various sensing devices beyond chemical sensors. © 2013 American Institute of Physics. [<http://dx.doi.org/10.1063/1.4794147>]

During the past decades, field effect transistor (FET) sensors, in which the surface potential of the conduction channel is modulated by charged molecules, have attracted a great deal of attention for chemical and biological applications.^{1,2} Recently, it has been shown that the use of nanoscale materials such as silicon nanowires (SiNWs) can significantly improve the sensitivity of FET sensors,^{3,4} allowing detection of a very low concentration of analytes. Due to the large surface-to-volume ratio,⁵ nanoscale Si FETs are expected to have excellent sensitivity. Label-free, direct electrical detection is another advantage of FET sensors. By exploiting these attractive features, SiNW FETs have been demonstrated for the detection of ions,^{3,4,6} proteins,^{3,4,7} DNA,⁸ virus,⁹ and cells.¹⁰ However, complex procedures for integrating nanowires into a nanosensor remains an obstacle for widespread applications. The “bottom up” approach requires assembly of nanowires grown from chemical vapor deposition (CVD),¹¹ which not only involves CMOS incompatible processes but also suffers from difficulty in precisely positioning of nanowires. Metal contamination from catalysts used during CVD growth is another disadvantage. Alternative “top-down” methods are proposed to overcome these shortcomings, providing CMOS compatibility and precise control of nanowire position.^{4,12–14} The “top-down” approaches require complex, multiple fabrication steps for nanowire patterning, etching, and doping.

In this work, we report a single-step approach to fabricate boron-doped silicon wires with diameters of a few hundred nm for Si FET sensors. Boron-doped Si wires are deposited using laser direct writing in combination with CVD which we previously demonstrated for deposition of intrinsic SiNWs.¹⁵ The unique feature of the fabricated Si wires is that they can have very rough surface which is beneficial for sensing applications due to its large surface area. In addition, our approach features excellent control of position, orientation, and length, *in situ* doping, and catalyst-free growth. The direct deposition of semiconductor wires on an

insulating SiO₂ surface provides a platform ready for subsequent device fabrication. Furthermore, the technique have potential for fabricating sensor arrays with different doping concentrations, which would enable multiplexed detection of analytes.⁷ Laser direct written Si FETs are employed to detect the proton concentration (pH) of an aqueous solution. The excellent sensitivity of our sensor device demonstrates that our approach offers a simple and promising way to fabricate highly sensitive Si FET sensors.

The fabrication starts with deposition of boron-doped Si wires using the laser direct write CVD method. A schematic depicting the technique is shown in Fig. 1(a). A femtosecond, mode-locked Ti:sapphire laser with a wavelength of 800 nm and about 100 fs pulse duration was frequency-doubled to 400 nm and used to locally heat an area on a substrate. To achieve small dimensions, the laser beam was focused on a diffraction-limited spot as small as 250 nm using high numerical aperture Fresnel phase zone plates.¹⁵ The substrate is a 200 nm-thick silicon dioxide top layer over a 200 nm-thick polycrystalline silicon (poly-Si) layer on quartz. The silicon dioxide top layer electrically isolated the deposited Si wires from the substrate, and the poly-Si layer serves as a means for absorbing laser radiation. The substrate was located in a vacuum chamber at a pressure between 30 and 40 Torr with flow of 10% silane in argon and 100 ppm diborane in hydrogen. In order to obtain a low doping concentration of a Si wire desirable for high sensitivity,¹⁶ we lightly doped our Si wires with a SiH₄:B₂H₆ mass flow ratio of 6000:1. The reactive gases decomposed on the laser spot due to the thermal energy of the laser and p-type silicon was deposited. In the meantime, movement of the piezoelectric stage holding the substrate created silicon lines in a desired pattern.

Figures 1(b)–1(d) show scanning electron microscope (SEM) images of Si wires synthesized using laser direct writing. The length of a Si wire can be precisely controlled up to 200 μm, which is the maximum travel distance of the piezoelectric stage, with a precision determined by the piezoelectric stage. Si wires with different surface morphologies were produced by controlling the polarization of the laser beam,

^{a)} Author to whom correspondence should be addressed. Electronic mail: xxu@purdue.edu.

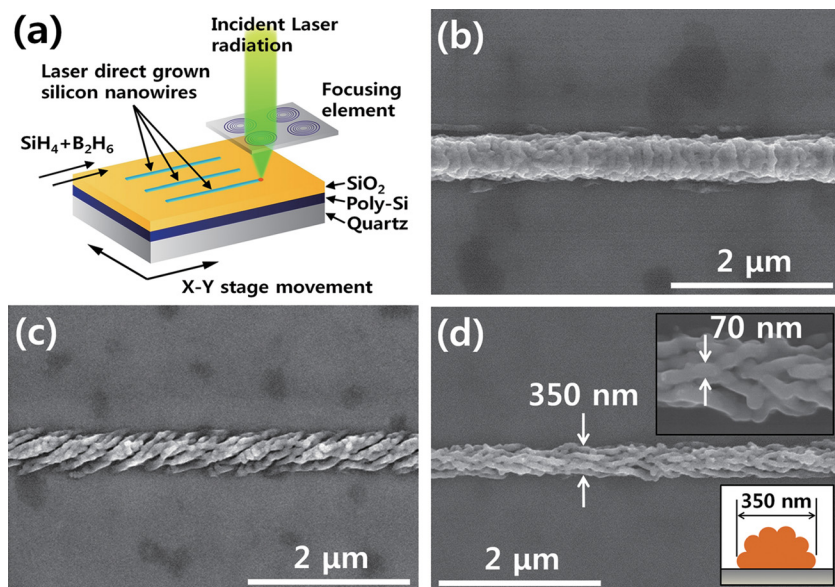


FIG. 1. (a) Schematic diagram of laser direct writing of silicon wires. A laser beam (green) is focused on a localized spot (red dot) where a silicon wire is synthesized. Fresnel phase zone plates were used to focus the laser beam. (b)–(d) SEM images of laser direct written silicon wires with (b) horizontally polarized light and (c) and (d) circularly polarized light. The upper inset in (d) shows a high resolution SEM image of the wire in (d). The lower inset in (d) shows a schematic cross section of the wire in (d).

analogous to the formation of laser induced surface structures.¹⁷ The wire in Fig. 1(b) was created with horizontally polarized light, while the wires in Figs. 1(c) and 1(d) were created with circularly polarized light. For sensor fabrication, we chose the wire shown in Fig. 1(d) which is about 350 nm wide and has a rough surface since its large surface area is desirable for high sensitivity. The wire is an agglomerate of 70 nm-thick nanowires as shown in the upper inset of Fig. 1(d). Using the cross section in the lower inset of Fig. 1(d), we calculated the surface-to-volume ratio of our wire to be 1.4 times that of a smooth, cylindrical wire of the same thickness. However, if we consider the 350 nm wire consisting of strands of 70 nm wires, which is closer to what is shown in the upper inset of Fig. 1(d), the surface-to-volume ratio will be about 5 times that of the smooth nanowire. Therefore, the actual surface-to-volume ratio can be between 1.4 and 5 times that of a smooth wire. It is also worth noting that our Si wires are composed of poly-Si. Poly-Si NW FET sensors have been found to be very promising as sensitive biosensors.^{12,14}

The laser direct written wires were annealed at 1000 °C in argon for 30 min to activate dopant atoms. Nickel (Ni) contacts were then formed by standard photolithography and electron beam evaporation. Immediately before Ni evaporation, the photoresist-patterned device chip was etched in buffered oxide etch for 5 s to remove native oxide on the surface. The metallized nanosensor was annealed using rapid thermal annealing at 400 °C in forming gas (4% H₂/96% N₂)

for 2 min to form low-resistance NiSi contacts at the interfaces between the Si wires and the Ni electrodes.¹¹ The electrical contacts were subsequently passivated from electrolyte by deposition of an AZ1518 photoresist layer. Figure 2(a) shows an optical image of a typical device with four Si wires aligned horizontally, illustrating that our laser direct write method is capable of producing a position-controlled array of Si wires. In the device, the separation between source/drain contacts is 20 μm and the width of the vertical channel exposed to an electrolyte solution in pH sensing experiment is 10 μm. Figure 2(b) shows a SEM image of a sensor device without a passivation layer.

To demonstrate pH sensing, laser direct written FET sensors were characterized in standard pH buffer solutions (pH 3–10, EMD Chemicals, Inc.). We used the solution-gate approach where a gate voltage is applied by a Ag/AgCl reference electrode (RE-5B, BASi) immersed in electrolyte. A custom-made solution chamber made of silicon rubber was placed on the sensor chip to hold pH solutions. Electrical measurement was performed at a room temperature on a probe-station using a Keithley 4200-SCS semiconductor parameter analyzer and the low-frequency noise in our device was measured using an Agilent 35670 A spectrum analyzer.

Figure 3(a) shows the drain current (I_D) dependence on the gate voltage (V_G) with a constant drain voltage (V_D) of 100 mV in solutions with pH values varying from 3 to 10. Consistent with p-type accumulation behavior, the

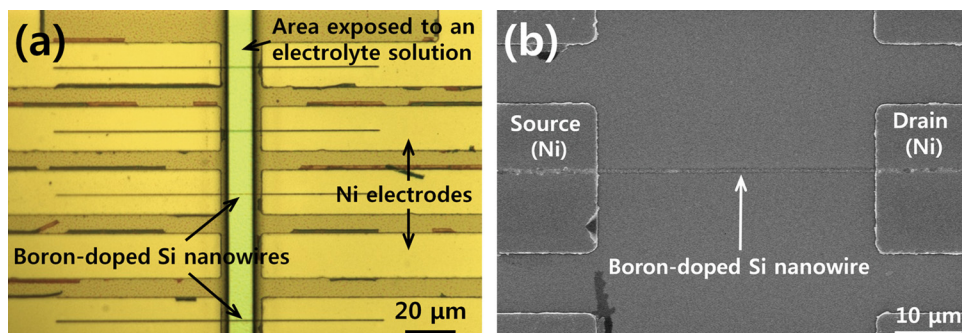


FIG. 2. (a) Optical image of a laser direct written Si FET device. (b) SEM image of a Si FET device without a passivation layer.

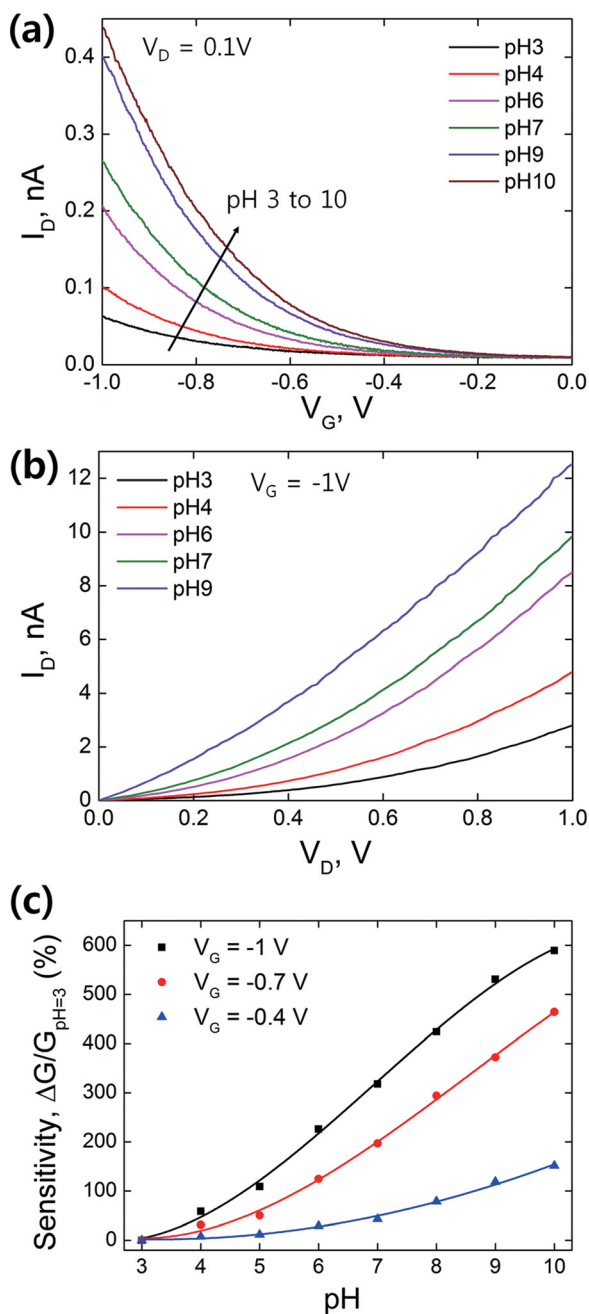


FIG. 3. Electrical response of a laser direct written Si FET sensor in different pH solutions. (a) I_D - V_G characteristics with a constant V_D of 0.1 V at pH values ranging from 3 to 10. (b) I_D - V_D characteristics with a constant V_G of -1 V at pH values ranging from 3 to 9. (c) Device sensitivity as a function of pH value at $V_G = -1$, -0.7 , and -0.4 V. Solid lines are guide to the eye.

conductance of the device increases with a negative gate voltage. As pH increases, the source-drain conduction increases as well. This is the expected behavior of a p-type Si FET. Hydroxyl ($-\text{OH}$) groups on the oxide surface of the Si wire can be protonated or deprotonated in electrolyte depending on the pH value of the solution,^{18,19} which causes changes in the surface charge and in turn modulates the conductance of the Si wire. As a result of the additional gating effect from the surface charges, hole carriers in the p-type Si wire are depleted and the conductance of the wire decreases at low pH, and vice versa, at high pH. Figure 3(b) shows the drain current (I_D) versus the drain voltage (V_D) with a

constant gate voltage (V_G) of -1 V at different pH values. The I_D value at $V_D = 0.5$ V increases from 0.6 nA at pH 3 to 4.9 nA at pH 9, demonstrating that our device is highly sensitive to solution pH. The small nonlinearity observed in the I_D - V_D curves is attributed to slightly non-ohmic contacts between the Si wire and the source/drain electrodes. During the measurement, the leakage current in aqueous solution between gate and source/drain electrodes was kept smaller than 0.02 nA, which indicates that the passivation layer over the source/drain electrodes effectively suppressed the gate leakage. However, the leakage current started to increase when V_G became smaller than -1 V.

An electrostatic potential drop, φ , in electrolyte at an electrolyte-silicon interface is described by the site-binding model and the electrical double layer theory:¹⁹ $\varphi = (2.303kT/q)(\beta/(\beta+1))(pH_{pzc} - pH)$ with k as the Boltzmann constant, T as the absolute temperature, q as the unit of charge, β as a dimensionless sensitivity parameter, and pH_{pzc} as the pH at the point of zero charge. According to this equation, a change in pH induces an alteration of the surface potential of the Si wire, thus, causing a shift in the I_D - V_G curve. The prefactor in the equation is the well-known Nernst value of 59 mV/pH, which usually limits the maximum shift of the I_D - V_G curve. In Fig. 3(a), parallel shifts of the I_D - V_G curves are observed. By comparing V_G values of the curves at a constant I_D of 0.2 nA, we roughly estimate the shift of the curves between pH 6 and 10 to be ~ 48 mV/pH, which is in good agreement with previously reported values for solution-gated pH sensors.²⁰

The sensitivity of a Si FET sensor is defined as normalized conductance change, $\Delta G/G_0 = (G - G_0)/G_0$.^{4,16,21} Figure 3(c) shows the sensitivity of our device, $\Delta G/G = (G - G_{pH=3})/G_{pH=3}$, as a function of pH at different V_G values. $\Delta G/G$ is about 150% at pH 10 with $V_G = -0.4$ V and increases as V_G becomes more negative. With $V_G = -1$ V, $\Delta G/G$ is about 600% at pH 10, which is comparable or superior to those reported for sensors made from CVD grown nanowires. Cui *et al.*,³ for example, reported $\sim 100\%$ of $\Delta G/G$ between pH 2 and 9, while Gao *et al.*²¹ reported $\sim 600\%$ between pH 4 and 9. We believe that the high sensitivity of our sensor is due to the rough surface and the low doping concentration of the Si wire. Since the Debye screening length of silicon, $L_D = (\epsilon_{Si}kT/q^2N_A)^{1/2}$, is longer as a doping concentration, N_A , is lower,²² the reduced screening of carriers in the Si wire makes the gating effect of ions on the surface more effective. The signal-to-noise ratio (SNR) of our sensor was obtained by measuring the low-frequency noise of the device. The SNR can be given by²³

$$SNR = \frac{\Delta\psi_0}{\sqrt{\ln(f_2/f_1)}} \frac{g_m(V_G)}{\sqrt{S_I(f = 1\text{Hz})}}, \quad (1)$$

where f_1 and f_2 are two corner frequencies of the measurement bandwidth, $\Delta\psi_0$ is the measured shift of the surface potential on the Si wire, S_I is the current noise power spectral density, and g_m is the transconductance. The voltage noise power spectral density S_V was measured with $V_D = 0.1$ V and $V_G = -1$ V in a pH 6 solution (titrated using sodium hydroxide from 50 mM potassium hydrogen phthalate, the Debye length²⁴ $\lambda_D = \sim 0.85$ nm) and S_I at 1 Hz was calculated to be

$9.4 \times 10^{-26} \text{ A}^2/\text{Hz}$ from the relation $S_I = S_V/R^2$. Using $\ln(f_2/f_1) = 1$ and $\Delta\psi_0 = 48 \text{ mV/pH}$, the SNR of our device was determined to be $\sim 160/\text{pH}$ and this corresponds to the noise equivalent pH change of 0.006. Therefore, the detection limit of our sensor is 0.6% of a pH change. The denominator in Eq. (1) is the root-mean-square current noise amplitude,²³ which can be used as a direct indication of the error in our device, and is calculated to be $3.1 \times 10^{-13} \text{ A}$ at $V_D = 0.1 \text{ V}$ and $V_G = -1 \text{ V}$. Considering FET nanosensors is known to have lower sensitivity in the linear transport regime,²¹ if V_G further decreases to the linear regime, $\Delta G/G$ is expected to decrease. Thus, operating the nanosensor with a proper gate voltage is another important factor for high sensitivity.

In summary, we have demonstrated a single-step approach to fabricate Si FET sensors for pH detection. Our approach utilizes a laser to fabricate p-type Si wires at a desired location on an insulating surface, simplifying overall fabrication processes and thus facilitating integration of Si wires into sensor devices. Moreover, these wires are rough, therefore, even if the diameters of the wires are $\sim 300 \text{ nm}$, they still provide large surface area for high sensitivity. The fabricated Si FET sensors were shown to have excellent sensitivity to solution pH. Our approach can be easily extended for other sensing applications by proper surface functionalization. More generally, we expect that our approach could be a promising alternative for fabrication of many types of Si devices.

We acknowledge the support of the Defense Advanced Research Projects Agency (Grant No. N66001-08-1-2037) and the National Science Foundation (Grant No. CMMI-1120577).

¹M. J. Schöning and A. Poghosian, *Analyst* **127**, 1137 (2002).

²P. Bergveld, *Sens. Actuators, B* **88**, 1 (2003).

³Y. Cui, Q. Wei, H. Park, and C. M. Lieber, *Science* **293**, 1289 (2001).

⁴E. Stern, J. F. Klemic, D. A. Routenberg, P. N. Wyrembak, D. B. Turner-Evans, A. D. Hamilton, D. A. LaVan, T. M. Fahmy, and M. A. Reed, *Nature* **445**, 519 (2007).

⁵Y. Chen, X. Wang, M. K. Hong, S. Erramilli, P. Mohanty, and C. Rosenberg, *Appl. Phys. Lett.* **91**, 243511 (2007).

⁶Y. Chen, X. Wang, S. Erramilli, P. Mohanty, and A. Kalinowski, *Appl. Phys. Lett.* **89**, 223512 (2006).

⁷G. Zheng, F. Patolsky, Y. Cui, W. U. Wang, and C. M. Lieber, *Nat. Biotechnol.* **23**, 1294 (2005).

⁸J.-I. Hahm and C. M. Lieber, *Nano Lett.* **4**, 51 (2004).

⁹F. Patolsky, G. Zheng, O. Hayden, M. Lakadamyali, X. Zhuang, and C. M. Lieber, *Proc. Natl. Acad. Sci. U.S.A.* **101**, 14017 (2004).

¹⁰F. Patolsky, B. P. Timko, G. Yu, Y. Fang, A. B. Greytak, G. Zheng, and C. M. Lieber, *Science* **313**, 1100 (2006).

¹¹F. Patolsky, G. Zheng, and C. M. Lieber, *Nat. Protoc.* **1**, 1711 (2006).

¹²C.-Y. Hsiao, C.-H. Lin, C.-H. Hung, C.-J. Su, Y.-R. Lo, C.-C. Lee, H.-C. Lin, F.-H. Ko, T.-Y. Huang, and Y.-S. Yang, *Biosens. Bioelectron.* **24**, 1223 (2009).

¹³A. Gao, N. Lu, P. Dai, T. Li, H. Pei, X. Gao, Y. Gong, Y. Wang, and C. Fan, *Nano Lett.* **11**, 3974 (2011).

¹⁴M. M. A. Hakim, M. Lombardini, K. Sun, F. Giustini, P. L. Roach, D. E. Davies, P. H. Howarth, M. R. R. de Planque, H. Morgan, and P. Ashburn, *Nano Lett.* **12**, 1868 (2012).

¹⁵J. I. Mitchell, S. J. Park, C. A. Watson, P. Srisungsitthisunti, C. Tansarawiput, M. Qi, E. A. Stach, C. Yang, and X. Xu, *Opt. Eng.* **50**, 104301 (2011).

¹⁶P. R. Nair and M. A. Alam, *IEEE Trans. Electron Devices* **54**, 3400 (2007).

¹⁷A. Borowiec and H. K. Haugen, *Appl. Phys. Lett.* **82**, 4462 (2003).

¹⁸D. E. Yates, S. Levine, and T. W. Healy, *J. Chem. Soc., Faraday Trans. 1* **70**, 1807 (1974).

¹⁹L. Bousse, N. F. De Rooij, and P. Bergveld, *IEEE Trans. Electron Devices* **30**, 1263 (1983).

²⁰O. Knopfmacher, A. Tarasov, W. Fu, M. Wipf, B. Niesen, M. Calame, and C. Schönenberger, *Nano Lett.* **10**, 2268 (2010).

²¹X. P. A. Gao, G. Zheng, and C. M. Lieber, *Nano Lett.* **10**, 547 (2010).

²²S. M. Sze and K. K. Ng, *Physics of Semiconductor Devices* (John Wiley & Sons Inc., Hoboken, 2007), p. 85.

²³N. K. Rajan, D. A. Routenberg, and M. A. Reed, *Appl. Phys. Lett.* **98**, 264107 (2011).

²⁴J. N. Israelachvili, *Intermolecular and Surface Forces*, 3rd ed. (Elsevier, Amsterdam, 2011), p. 322.